PAPER

NJC
www.rsc.org/njc

# Halogenated silicon(IV) phthalocyanines with axial poly(ethylene glycol) chains. Synthesis, spectroscopic properties, complexation with bovine serum albumin and *in vitro* photodynamic activities†

**Jian-Dong Huang,[ab] Shuangqing Wang,[a] Pui-Chi Lo,[a] Wing-Ping Fong,[c] Wing-Hung Ko[d] and Dennis K. P. Ng*[a]**

[a] *Department of Chemistry, The Chinese University of Hong Kong, Shatin, N.T., Hong Kong, China. E-mail: dkpn@cuhk.edu.hk*
[b] *Institute of Research on Functional Materials, Department of Chemistry, Fuzhou University, Fuzhou 350002, China*
[c] *Department of Biochemistry, The Chinese University of Hong Kong, Shatin, N.T., Hong Kong, China*
[d] *Department of Physiology, The Chinese University of Hong Kong, Shatin, N.T., Hong Kong, China*

***Received* (*in Montpellier, France*) *11th July 2003, Accepted 13th November 2003***
***First published as an Advance Article on the web 27th January 2004***



A new series of unsubstituted and halogenated silicon(IV) phthalocyanines with two axial poly(ethylene glycol) (PEG) chains having an average molecular weight of 550 or 750 ($PEG_{550}$ or $PEG_{750}$) have been synthesised by treating the corresponding silicon phthalocyanine dichloride with PEG methyl ether in the presence of NaH. The compounds have been unambiguously characterised with $^1$H NMR and MALDI-TOF mass spectrometry. With two bulky polymeric substituents, the compounds are essentially non-aggregated in common organic solvents. The longer $PEG_{750}$ chain enhances the hydrophilicity of the phthalocyanine ring and is more effective to prevent aggregation and fluorescence quenching by $Cu(OAc)_2$. Substitution with heavier halogen atoms on the periphery of the ring leads to a reduction in fluorescence emission and an increase in singlet oxygen quantum yield, as a result of heavy atom effect. The compounds $Si(PcX_8)(PEG_{750})_2$ [X = H (**4b**), Cl (**4c**), Br (**4d**)] are photocytotoxic towards HepG2 human hepatocarcinoma cells and J774 mouse mammary tumour cells. Although halogenation results in an increase in singlet oxygen quantum yield, the general photocytotoxicity follows the order **4b** > **4d** > **4c**. This can be attributed to the opposite effect of aggregation, which follows the order **4a** < **4b** < **4c** in the growth medium. The interactions of **4b**–**d** with bovine serum albumin (BSA) have also been investigated by a fluorescence quenching method and a non-covalent conjugate of **4b** and BSA has been prepared. Conjugation with BSA leads to a higher photocytotoxicity against J774 cells, which have a BSA-loving macrophage origin.

## Introduction

Photodynamic therapy (PDT) is a promising approach for the treatment of cancer and certain non-cancerous conditions that involve overgrowth of unwanted or abnormal cells.[1] The treatment involves systemic administration of a photosensitising agent, which has selective affinity for malignant tissues and produces reactive oxygen species (ROS), such as singlet oxygen, when excited by red light of appropriate power. The therapeutic effect depends greatly on the behaviour of the photosensitisers. Photofrin®, which is a complex mixture of hematoporphyrin derivatives, is still widely used clinically despite deficiencies such as complex composition, poor absorption of tissue-penetrating red light, and prolonged retention. As a result, there has been a great demand for new photosensitisers that show superior efficiency and fewer side effects.[2] Owing to the desirable photophysical and hotochemical properties, ease of chemical modification, and low dark toxicity, phthalocyanines are promising candidates for this application. Substantial progress has recently been made in the development of phthalocyanine-based photosensitisers.[2,3]

To increase drug circulating half-life and uptake by abnormal tissues, poly(ethylene glycol) (PEG) has been widely used as a pharmaceutical vehicle.[4] While a substantial number of PEG-derivatised (or pegylated) drugs have been reported, conjugation of this polymeric material to photosensitisers for targeted PDT remains little studied.[5,6] *m*-Tetrahydroxyphenylchlorin (mTHPC), in particular, has been examined for the effects of pegylation.[6] It has been found that the biodistribution of the pegylated and non-pegylated mTHPC is remarkably different and the former generally exhibits enhanced photosensitising properties compared to the latter. Although phthalocyanines substituted with PEG chains on the peripheral positions have long been known, mainly for their liquid crystalline properties,[7] reports on the photodynamic activities of pegylated phthalocyanines are extremely rare.[8] Bellemo and co-workers reported a silicon(IV) 2,3-naphthalocyanine with two axial $PEG_{1900}$ chains, which showed little tumour selectivity and no phototherapeutic activity towards a MS-2 fibrosarcoma transplanted in Balb/c mice.[8a] In contrast, the aluminum analogue $AlPc(PEG_{2000})$ was found to be highly photocytotoxic against the EMT-6 mouse mammary tumour cells and the colon carcinoma Colo-26.[8b] It was found that the additional hydrophilic axial ligand changed the *in vitro* and *in vivo* kinetics, but did not reduce the photodynamic activity of the parent photosensitiser. Non-covalent

† Dedicated to Prof. Malcolm L. H. Green on the occasion of his retirement, with our warmest congratulations.

DOI: 10.1039/b307934a

encapsulation of phthalocyanines in PEG-coated poly(lactic acid) nanoparticles and PEG-liposomes has also been reported and the efficiency of these delivery systems has been evaluated.[9] We have recently employed PEG as a dispersing agent to promote the formation of monomeric phthalocyanine in water.[10] We describe herein the synthesis, spectroscopic properties, and *in vitro* photodynamic activities of a series of silicon(IV) phthalocyanines covalently linked with two short PEG chains, namely $PEG_{550}$ or $PEG_{750}$, at the axial positions.[11] Their complexation with bovine serum albumin (BSA) and the effects of halogen substitution on the PDT efficiency are also reported.

## Results and discussion

### Preparation and characterisation

Scheme 1 shows the synthetic pathway to the PEG-containing phthalocyanines **4a**–**d**. The unsubstituted and halogenated derivatives were prepared in a similar manner. Starting from the dichloro- (**1b**) or dibromophthalonitrile (**1c**), bubbling of dry ammonia in the presence of NaOMe led to the respective 1,3-diiminoisoindoline **2b** or **2c**. Upon treatment with $SiCl_4$ in quinoline, these compounds were converted to the corresponding silicon phthalocyanines **3b** and **3c**. Due to their poor solubility in common organic solvents, the macrocycles could only be purified by Soxhlet extraction.

Treatment of **3a**–**c** with $PEG_{550}$ or $PEG_{750}$ methyl ether in the presence of NaH led to axial substitution, giving **4a**–**d** in moderate yields (Scheme 1). These polymeric materials are highly soluble in various organic solvents and could be purified readily by column chromatography. Reaction of diiodophthalonitrile with ammonia also afforded a 1,3-diiminoisoindoline, but attempts to prepare the octaiodo analogue of **4a**–**d** following the same route were not successful. The $^1$H NMR spectrum of the product showed several signals instead of a singlet in the aromatic region. This indicated that some of the iodo groups were cleaved under the strong basic conditions.

Apart from the signal(s) for the phthalocyanine ring protons, the $^1$H NMR spectra of **4a**–**d** showed up to 8 well-separated and upfield-shifted virtual triplets for the chain methylene protons nearest to the ring centre. Due to the shielding effect by the ring current, these signals were significantly shifted upfield (up to $\delta - 1.9$). Compounds **4b**–**d** were also characterised by MALDI-TOF mass spectrometry.[11] The spectrum of **4b** showed two major envelopes for the molecular ion $M^+$ and the $[M - O(CH_2CH_2O)_nMe]^+$ fragment, each separated by 44 mass units corresponding to the repeating unit of PEG. These signals were relatively weak for the chloro and bromo analogues, for which an envelope due to the $Na^+$ adduct of the $-O(CH_2CH_2O)_nMe$ fragment appeared as the base peak.

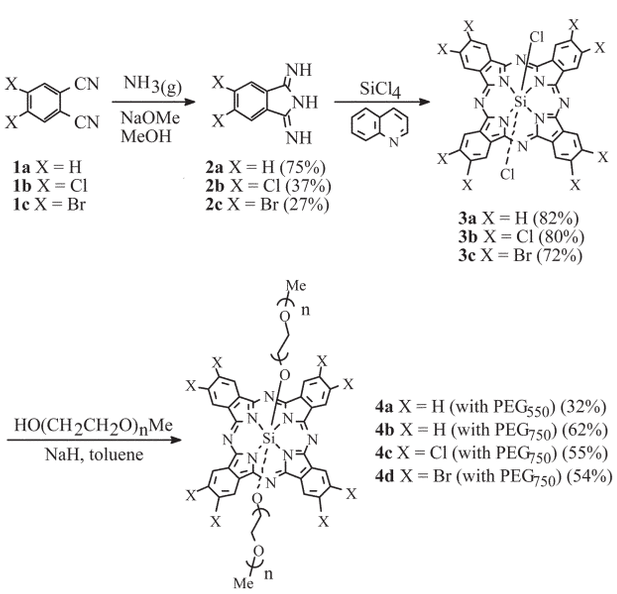


**Scheme 1** Preparation of pegylated phthalocyanines.

### Electronic absorption and photophysical properties

The electronic absorption spectra of **4a**–**d** in *N*,*N*-dimethylformamide (DMF) were typical for non-aggregated phthalocyanines, showing a B (or Soret) band at 354–360 nm, an intense and sharp Q band at 671–682 nm, together with two vibronic bands at 604–613 and 641–652 nm. All these absorptions shifted slightly to the red upon halogenation as shown in Table 1. Monomeric spectra were also observed for these compounds in MeOH, EtOH, tetrahydrofuran (THF) and $CHCl_3$. To briefly examine the aggregation behaviour, the absorption spectra of **4a** and **4b** in DMF were recorded in different concentrations. It was found that **4a** did not follow the Lambert–Beer law at concentrations higher than *ca.* 5 μM, while **4b** gave a perfect straight line in the plot of absorbance *vs.* concentration up to *ca.* 10 μM.[12] This observation indicates that the longer $PEG_{750}$ is more effective than $PEG_{550}$ to hinder the aggregation of phthalocyanine. The longer $PEG_{750}$ also enhances the hydrophilicity of the phthalocyanine ring. While **4a** did not give a noticeable Q band absorption and fluorescence emission in water, the absorption spectrum of **4b** in water showed a rather intense Q band at 682 nm. Upon excitation at 610 nm, this compound also showed a fluorescence emission at 687 nm with a quantum yield of 0.25. It is worth noting that due to the strong aggregation and hydrophobic interactions, fluorescence of phthalocyanines is rarely observed in aqueous media.[13] The chloro and bromo analogues **4c** and **4d** have a lower solubility in water. The absorption spectra in water showed broad Q bands due to the aggregated species and no fluorescence signal was observed.

Compounds **4a** and **4b** were highly fluorescent in DMF and the data are summarised in Table 1. Upon addition of $Cu(OAc)_2$, which acts as a quencher, the fluorescence intensity of these compounds decreased gradually and the data could be analysed by the Stern–Volmer equation: $I_o/I = 1 + K_{SV}[Q]$, where $I_o$ and $I$ are the fluorescence intensities in the absence and presence of the quencher, respectively, [Q] is the concentration of the quencher, and $K_{SV}$ is the Stern–Volmer quenching constant. Under similar conditions ([fluorophore] = 1.2–1.6 μM in DMF, [Q] varied from 0 to 3.7 mM), both compounds gave a linear Stern–Volmer plot from which the value of $K_{SV}$ was found to be 590 $M^{-1}$ for **4a** and 310 $M^{-1}$ for **4b**. This shows that the longer $PEG_{750}$ imposes a more hindered environment to prevent the approach of the quencher.

To evaluate the photosensitising efficiency of these PEG-containing phthalocyanines, their singlet oxygen quantum yields ($\Phi_\Delta$) were determined by a steady-state method using 1,3-diphenylisobenzofuran (DPBF) as the scavenger. The concentration of the quencher was monitored spectroscopically at 411 nm with time, from which the values of $\Phi_\Delta$ could be determined.[14] As shown in Table 1, the value of $\Phi_\Delta$ follows the

**Table 1** Electronic absorption and photophysical data for **4a**–**d** in DMF

| Compound | $\lambda_{max}$/nm | $\lambda_{em}$/nm[a] | $\Phi_F$[b] | $\Phi_\Delta$[c] |
|---|---|---|---|---|
| **4a** | 354, 604, 641, 671 | 677 | 0.82 | 0.16 |
| **4b** | 355, 606, 644, 672 | 676 | 0.80 | 0.20 |
| **4c** | 358, 611, 650, 679 | 684 | 0.73 | 0.38 |
| **4d** | 360, 613, 652, 682 | 690 | 0.34 | 0.52 |

[a] Excited at 610 nm. [b] Relative to ZnPc ($\Phi_F = 0.30$ in 1-chloronaphthalene). [c] Relative to ZnPc ($\Phi_\Delta = 0.55$ in DMF).

order **4a** ≈ **4b** < **4c** < **4d**. The trend is in accord with the heavy atom effect, which suggests that substitution with heavy atoms enhances intersystem crossing, leading to a higher singlet oxygen quantum yield. This concomitantly decreases the fluorescence quantum yield as found for these compounds (Table 1).

### Interactions with BSA

BSA is a common protein carrier for anticancer drugs to improve their passive targeting properties.[15] With the goal of enhancing the biocompatibility and selectivity of these phthalocyanine-based photosensitisers, attempts were made to prepare the BSA conjugates of these dyes. To this end, we firstly investigated the interactions of **4b**–**d** with BSA by a fluorescence quenching method. Fig. 1 shows the change in fluorescence spectrum of BSA upon titration with **4d** in an aqueous solution containing 50 mM tris(hydroxymethyl)aminomethane and 0.1 M NaCl, which has been adjusted to pH 7.4 with HCl(aq) (Tris-HCl buffer). The emission band at 343 nm decreases in intensity and shifts gradually to 327 nm. As shown in the inset of Fig. 1, the quenching data follow the Stern–Volmer equation, giving a $K_{SV}$ of $3.9 \times 10^5$ $M^{-1}$. Compound **4c** behaved similarly except that the rate of quenching was significantly faster. At a phthalocyanine to BSA molar ratio of 5, for example, the $I_o/I$ value increased from 12 (for **4d**) to 40 (for **4c**). The Stern–Volmer plot, however, was curved upward, preventing the determination of the $K_{SV}$ value. The non-halogenated analogue **4b** could also quench the fluorescence of BSA, but interestingly two instead of one emission bands, at 339 and 372 nm, were observed during the titration. It seems that this compound interacts with BSA and changes its micro-environment in a different manner compared with the halogenated counterparts. The Stern–Volmer plot for this compound was also curved upward and the apparent rate of quenching lay between those of **4c** and **4d**.

In view of the strong interactions between these phthalocyanines and BSA, attempts were made to prepare their non-covalent conjugates. The **4b**-BSA conjugate was prepared by stirring a mixture of **4b** and BSA (with a molar ratio of 20) in a Tris-HCl buffer, followed by chromatography on a G-100 Sephadex column using aqueous $NH_4HCO_3$ (pH 8.3) as eluent. Fig. 2 shows the elution profile monitored by absorption (for the phthalocyanine absorption at 680 nm) and fluorescence (for the BSA emission at 340 nm) spectroscopy. For comparison, the elution profiles of pure **4b** and BSA were also obtained, which showed a maximum at an elution volume of 37 and 16 mL, respectively. Thus, it can be seen in Fig. 2 that at an elution volume of 16–17 mL, the fraction contains both

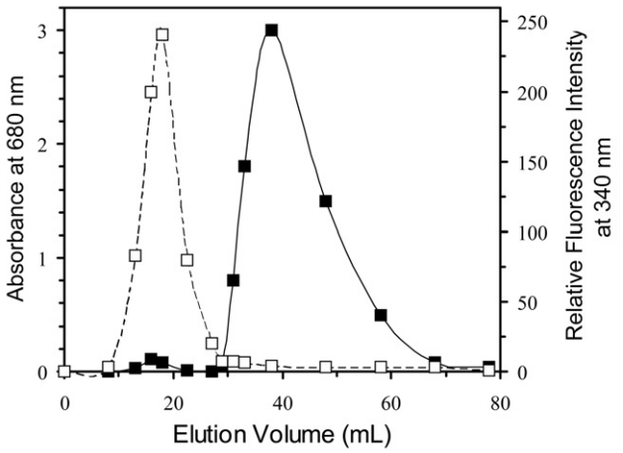


**Fig. 2** Elution profiles of **4b**-BSA as monitored by (■) absorbance at 680 nm and (□) fluorescence emission at 340 nm upon excitation at 280 nm.

phthalocyanine and BSA. Since a large excess of **4b** was used (as also shown in Fig. 2), it was expected that the fraction would be free from uncomplexed BSA. The protein content in the resulting conjugate was determined with the Bio-Rad protein assay kit using BSA as standard.[16] The concentration of **4b** was measured from the Q band absorbance in a diluted DMF solution ($\varepsilon_{672} = 2.1 \times 10^5$ $M^{-1}$ $cm^{-1}$). The molar ratio of **4b** to BSA was found to be *ca.* 1:1 in this conjugate. Attempts to prepare the BSA conjugates of **4c** and **4d** using a similar procedure were not successful. The phthalocyanines form large aggregates in the aqueous solution, of which the elution volumes (*ca.* 18–20 mL) are close to those of free BSA and the conjugates if formed, making separation a difficult task.

The absorption spectrum of **4b**-BSA in phosphate buffered saline (PBS) is given in Fig. 3, which also displays the spectrum of **4b** in PBS for comparison. The latter shows a very sharp and intense Q band at 681 nm, which strictly obeys the Lambert–Beer law up to 10 μM. The spectrum remained virtually unchanged upon standing for a few days. These observations suggest that the compound exists mainly in monomeric form and is stable in this solution. A rather sharp Q band was also seen for the conjugate, indicating that the phthalocyanine is also relatively non-aggregated in the conjugate.

### *In vitro* photodynamic activities

The photodynamic activities of **4b**–**d** and the BSA conjugate of **4b** against HepG2 and J774 cell lines were examined. Fig. 4

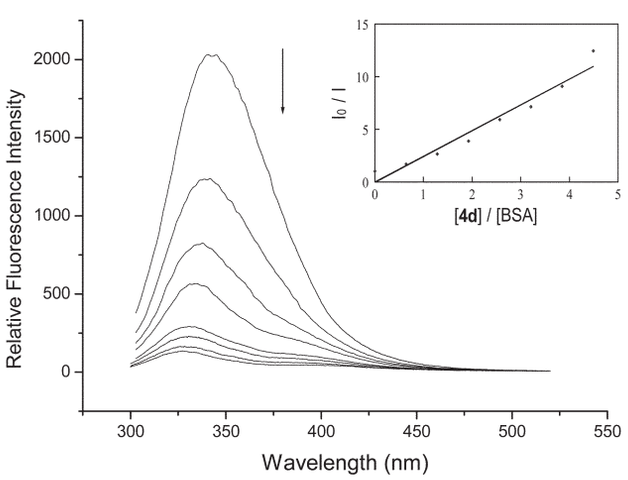


**Fig. 1** Change in fluorescence spectrum of BSA (6.4 μM, excited at 280 nm) in a Tris-HCl buffer upon titration with **4d**. The inset shows the corresponding Stern–Volmer plot.

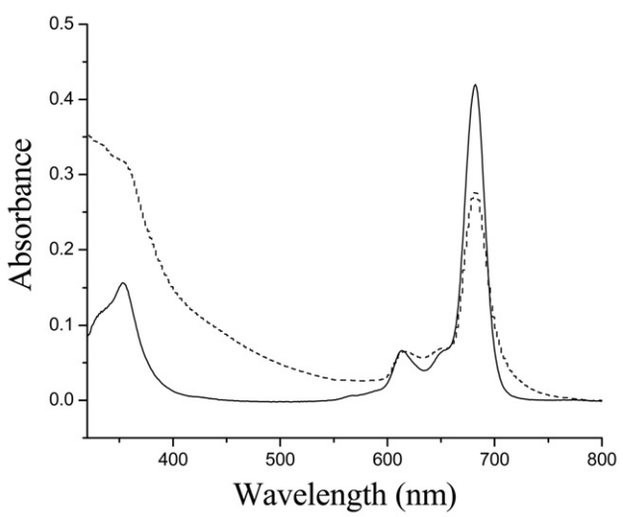


**Fig. 3** Absorption spectra of (—) **4b** (3.3 μM) and (---) **4b**-BSA conjugate (3.7 μM) in PBS.

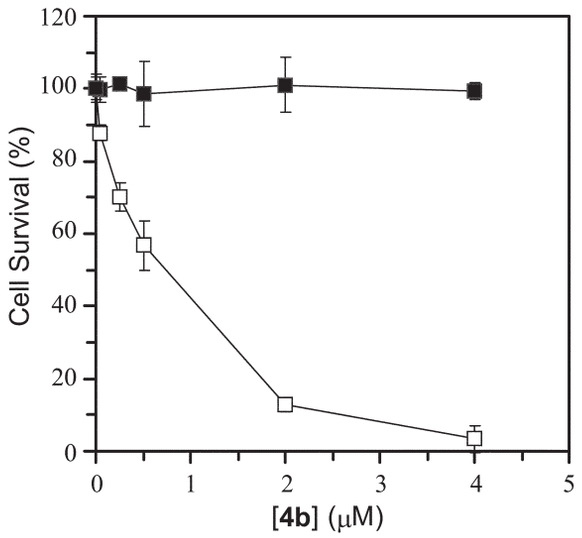


**Fig. 4** (■) Dark- and (□) photocytotoxicities of **4b** (in PBS) towards HepG2. For the latter, the cells were illuminated with a red light ($\lambda > 610$ nm, 40 mW cm$^{-2}$, 48 J cm$^{-2}$). Values are expressed as mean ± SD ($n \geq 3$).

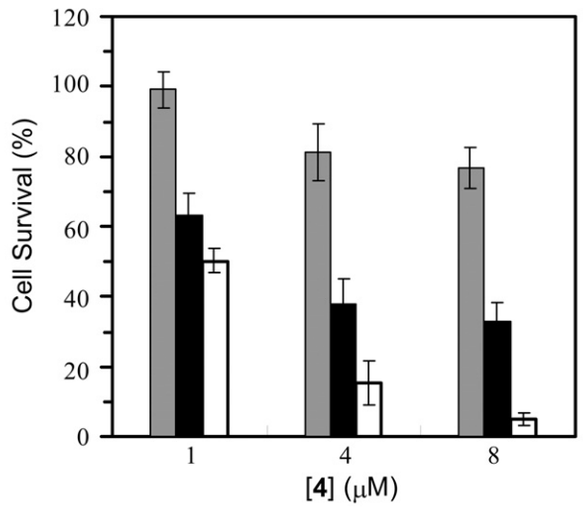


**Fig. 6** Comparison of the photocytotoxicities of (white) **4b**, (gray) **4c** and (black) **4d** (all in Cremophor EL emulsion) towards HepG2. The cells were illuminated with a red light ($\lambda > 610$ nm, 40 mW cm$^{-2}$, 48 J cm$^{-2}$). Values are expressed as mean ± SD ($n \geq 3$).

shows the survival curve for HepG2 using **4b** in PBS as the photosensitiser. While this system was essentially non-toxic in the absence of light, it exhibited a very high photocytotoxicity with a $LD_{50}$ (the extracellular dye concentration required to kill 50% of the cells) of 0.75 μM. All the cells were basically killed upon treatment with 4 μM of **4b**. Figs. 5(a) and (b) show the microscopic observations of the HepG2 cells after treatment with **4b**, both in the absence and presence of light. While no significant morphological change was observed in the absence of light, the cells became globular and shrunken after the photo-treatment, indicating cell death. The chloro and bromo analogues **4c** and **4d** had limited solubility in the medium and required Cremophor EL to formulate. These compounds were also non-toxic in the dark, but the photocytotoxicity was significantly lower than that of **4b** (also in Cremophor EL emulsion) and followed the order **4b** > **4d** > **4c**. The data are compared in Fig. 6. Compound **4b** exhibits a slightly higher photocytotoxicity in PBS solution than in Cremophor EL emulsion (Figs. 4 and 6).

The difference in photoactivity of these compounds can be attributed to different cellular uptake and extent of aggregation of the photosensitiser, and the effects of halogen substitution. Uptakes by HepG2 cells of **4b** in PBS and **4b–d** in Cremophor EL emulsion, after incubation for 2 h, were determined by absorption spectroscopy. Due to the weak fluorescence emission of **4c** and **4d**, the commonly used fluorescence method could not be applied. It was found that **4b** in PBS has the highest uptake (0.52 ± 0.04%), while the values for all three phthalocyanines in Cremophor EL emulsion are comparable (0.22 ± 0.05% for **4b**, 0.27 ± 0.07% for **4c**, 0.18 ± 0.08% for **4d**). The higher uptake of **4b** in PBS than in Cremophor EL emulsion may account for the higher photocytotoxicity. Fig. 7 shows a fluorescence microscopic image of HepG2 cells after 2 h incubation with **4b** in PBS. It is clear that the dye enters into the cell, causing substantial fluorescence in the cytoplasm. Fig. 8 shows the absorption spectra of **4b–d** in the growth medium in the presence of 1 mM Cremophor EL. It can be seen that while a sharp Q band appears for **4b**, this band is split and broaden upon halogenation. It appears that the content of monomeric phthalocyanine decreases in the order **4b** > **4c** > **4d**. By considering the fact that heavy atom substitution will enhance intersystem crossing, leading to a higher singlet oxygen quantum yield (see Table 1 for the data in DMF), it is expected that the bromo analogue **4d** may also be a better singlet oxygen generator in the medium. Since the

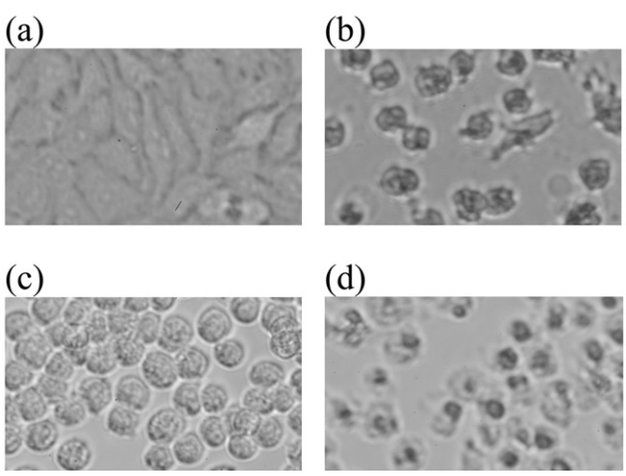


**Fig. 5** Microscopic views of HepG2 after incubation with **4b**: (a) without illumination; (b) upon illumination. The corresponding pictures for J774 are shown in (c) and (d), respectively.

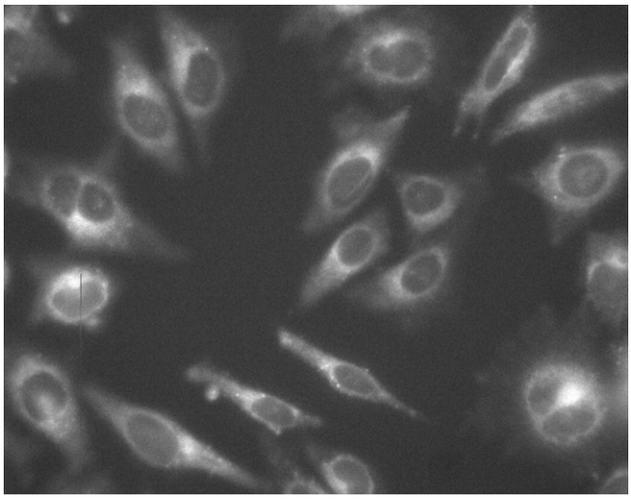

**Fig. 7** Fluorescence microscopic image of HepG2 after incubation with **4b** for 2 h.

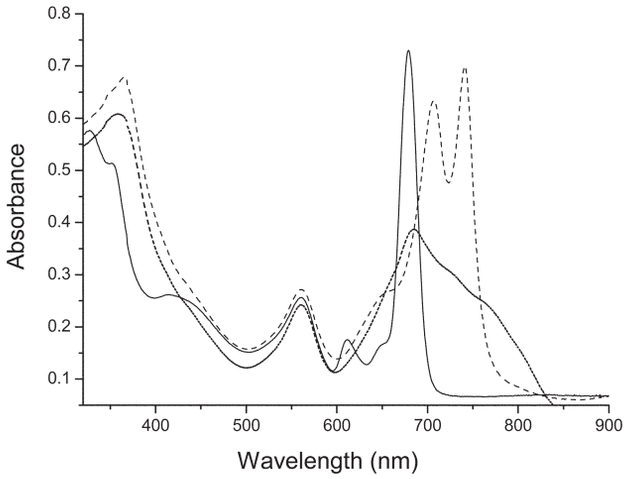


**Fig. 8** Absorption spectra of 4 μM of (—) **4b**, (---) **4c** and (···) **4d** in the growth medium in the presence of 1 mM Cremophor EL.

cellular uptake of these three compounds is comparable, the observed trend of photoactivity, **4b** > **4d** > **4c**, may be a result of the two opposing effects of aggregation and heavy atom substitution.

Compound **4b** in PBS was also highly photocytotoxic towards J774 cells (Fig. 9). The microscopic observation of these cells is shown in Figs. 5(c) and (d), in which the effect of light leading to cell death can be clearly seen. Because of the monocyte-macrophage origin of these cells, which have a high affinity for BSA,[17] the photodynamic activity of **4b**-BSA conjugate against J774 was also investigated. It can be seen in Fig. 9 that the conjugation leads to a substantial enhancement in photocytotoxicity. At a dose of 0.9 μM of **4b**, for example, the cell viability decreases from *ca.* 50% to 6%. The photoactivity of **4b–d** in Cremophor EL emulsion towards J774 was also compared. When 8 μM of photosensitiser was used, the cell viability was found to be 5% for **4b**, 81% for **4c**, and 23% for **4d**. The PDT efficiency thus again follows the order **4b** > **4d** > **4c**.

## Conclusion

We have prepared a series of four silicon(IV) phthalocyanines with two axial PEG chains and a BSA conjugate of one of these compounds, all of which are photocytotoxic against HepG2 and J774 cancer cells. Halogen substitution on the peripheral positions does not increase the PDT efficiency of the phthalocyanine core even though halogenated phthalocyanines have a higher singlet oxygen quantum yield. Other factors such as cellular uptake and the aggregation state of the photosensitiser also play an important role.

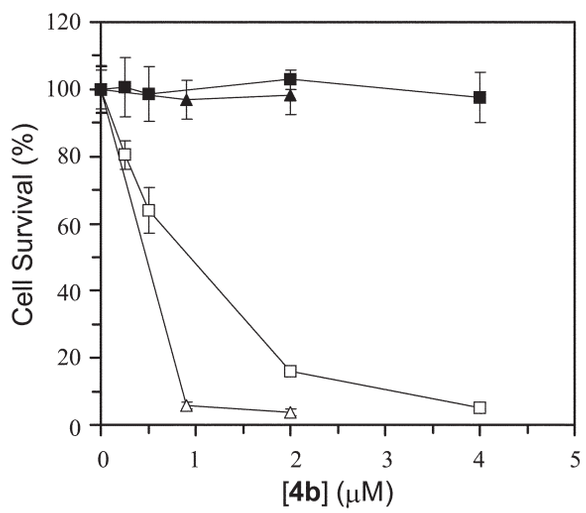


**Fig. 9** (Filled) Dark- and (open) photocytotoxicities of (■, □) **4b** and (▲, △) **4b**-BSA towards J774. Values are expressed as mean ± SD ($n \geq 3$).

## Experimental

### General

Reactions were performed under an atmosphere of nitrogen unless otherwise stated. Toluene and THF were distilled from sodium and sodium benzophenone ketyl, respectively. DMF was pre-dried over barium oxide and distilled under reduced pressure. Quinoline was pre-dried over anhydrous sodium sulfate and fractionally distilled from zinc dust *in vacuo*. Chromatographic purifications were performed on silica gel columns (Macherey-Nagel, 70–230 mesh) with the indicated eluents. All other solvents and reagents were of reagent grade and used as received. 4,5-Dichlorophthalonitrile (**1b**),[18] 4,5-dibromophthalonitrile (**1c**),[19] and silicon phthalocyanine dichloride (**3a**)[20] were prepared according to literature procedures.

$^1$H NMR spectra were recorded on a Bruker DPX 300 spectrometer (300 MHz) in $CDCl_3$ solutions unless otherwise stated. Chemical shifts are relative to internal $SiMe_4$ ($\delta$ 0). Electron impact (EI) mass spectra were measured on a Thermo Finnigan MAT 95 XL mass spectrometer. Matrix-assisted laser desorption/ionisation time-of-flight (MALDI-TOF) spectra were obtained on a Bruker bench TOF mass spectrometer equipped with a standard UV-laser desorption source, using 2,5-dihydroxybenzoic acid as matrix. Elemental analyses were performed by Medac Ltd., Brunel Science Centre, UK.

UV-Vis and steady-state fluorescence spectra were taken on a Cary 5G UV-Vis-NIR spectrophotometer and a Hitachi F-4500 spectrofluorometer, respectively. The fluorescence quantum yields were determined by the equation: $\Phi_{sample} = (F_{sample}/F_{ref})(A_{ref}/A_{sample})(n^2_{sample}/n^2_{ref})\Phi_{ref}$,[21] where $F$, $A$ and $n$ are the measured fluorescence (area under the emission peak), the absorbance at the excitation position (610 nm) and the refractive index of the solvent, respectively. Unsubstituted zinc(II) phthalocyanine (ZnPc) in 1-chloronaphthalene was used as the reference ($\Phi_F = 0.30$).[22] To minimise reabsorption of radiation by the ground-state species, the emission spectra were obtained in very dilute solutions where the absorbance at 610 nm was less than 0.03. Singlet oxygen quantum yields ($\Phi_\Delta$) were measured by the method of chemical quenching of DPBF described by Wöhrle and co-workers,[14] except that the light intensity of our system was not determined. All measurements were performed in DMF using ZnPc as a reference ($\Phi_\Delta = 0.55$).

### Syntheses

**Dichloro-1,3-diiminoisoindoline (2b).** Sodium (0.06 g, 2.61 mmol) was dissolved in methanol (50 mL), to which 4,5-dichlorophthalonitrile (**1b**; 1.05 g, 5.33 mmol) was added. Ammonia was bubbled at a moderate rate into this mixture at ambient temperature for 40 min. The mixture was then brought to reflux for 3 h with continued stirring and addition of ammonia. Upon cooling, the green solid formed was filtered and washed with diethyl ether. The crude product was further purified by recrystallisation from methanol to afford greenish yellow crystals (0.42 g, 37%). $^1$H NMR (DMSO-$d_6$) $\delta$ 8.4–9.1 (br s, 3 H, NH), 8.08 (s, 2 H, ArH). HRMS (EI) $m/z$ calcd for $C_8H_5{}^{35}Cl^{37}ClN_3$ ($M^+$) 212.9855, found 212.9857. Anal. calcd for $C_8H_5Cl_2N_3$: C, 44.89; H, 2.35; N, 19.63; found: C, 44.46; H, 2.36; N, 18.94.

**Dibromo-1,3-diiminoisoindoline (2c).** According to the above procedure, 4,5-dibromophthalonitrile (**1c**; 1.14 g, 3.99 mmol)

was mixed with sodium (0.06 g, 2.61 mmol) in methanol (50 mL). After being stirred at ambient temperature for 40 min under an ammonia atmosphere, the mixture was heated at 60 °C for 2 h with continued stirring and addition of ammonia. Upon cooling, the orange solid formed was filtered and washed with diethyl ether. The crude product was further purified by recrystallisation from methanol (0.32 g, 27%). $^1$H NMR (DMSO-$d_6$) $\delta$ 9.1–9.5 (br s, 3 H, NH), 8.25 (s, 2 H, ArH). HRMS (EI) $m/z$ calcd for $C_8H_5{}^{79}Br^{81}BrN_3$ ($M^+$) 302.8825, found 302.8823.

**Si(PcCl$_8$)Cl$_2$ (3b).** A mixture of dichloro-1,3-diiminoisoindoline (**2b**; 0.16 g, 0.75 mmol) and $SiCl_4$ (0.12 mL, 1.05 mmol) in quinoline (20 mL) was heated at reflux for 2 h. The mixture was then poured into benzene (80 mL) to give a blue paste, which was filtered and washed thoroughly with benzene, methanol and acetone. The resulting blue sold was then Soxhlet extracted with a mixture of these solvents plus $CHCl_3$ for 2 days to give a shiny blue solid (0.13 g, 80%).

**Si(PcBr$_8$)Cl$_2$ (3c).** A mixture of dibromo-1,3-diiminoisoindoline (**2c**; 0.76 g, 2.51 mmol) and $SiCl_4$ (0.50 mL, 4.36 mmol) in quinoline (35 mL) was heated at reflux for 1.5 h. By using the above work-up procedure, a shiny blue solid was obtained (0.55 g, 72%).

**Si(PcH$_8$)(PEG$_{550}$)$_2$ (4a).** A mixture of Si(PcH$_8$)Cl$_2$ (**3a**; 0.10 g, 0.16 mmol), $PEG_{550}$ methyl ether (average $M_n \approx 550$; 0.20 g, *ca.* 0.4 mmol) and NaH (20 mg, 0.83 mmol) in toluene (10 mL) was refluxed for 3 days. The solvent was then removed *in vacuo* and the residue was subjected to column chromatography using $CHCl_3$–EtOH (9:1) as eluent. The crude product was re-dissolved in ethyl acetate and the solution was extracted with water to remove the unreacted $PEG_{550}$ methyl ether. The organic portion was dried over anhydrous $MgSO_4$ and rotary evaporated to give a green solid (86 mg, 32%). $R_f$ [$CHCl_3$–EtOH (9:1)] = 0.55. $^1$H NMR $\delta$ 9.60–9.63 (m, 8 H, Pc–H$_\alpha$), 8.30–8.35 (m, 8 H, Pc–H$_\beta$), 3.51–3.63 (m, *ca.* 68 H, $CH_2$), 3.44 (vt, $J$ = 4.8 Hz, 4 H, $CH_2$), 3.36 (s, 6 H, Me), 3.17 (vt, $J$ = 4.8 Hz, 4 H, $CH_2$), 2.95 (vt, $J$ = 4.8 Hz, 4 H, $CH_2$), 2.43 (vt, $J$ = 4.8 Hz, 4 H, $CH_2$), 1.65 (vt, $J$ = 4.8 Hz, 4 H, $CH_2$), 0.38 (vt, $J$ = 5.7 Hz, 4 H, $CH_2$), −1.92 (vt, $J$ = 5.7 Hz, 4 H, $CH_2$).

**Si(PcH$_8$)(PEG$_{750}$)$_2$ (4b).** By using the above procedure, **3a** (0.64 g, 1.05 mmol) was treated with $PEG_{750}$ methyl ether (average $M_n \approx 750$; 1.79 g, *ca.* 2.4 mmol) and NaH (0.14 g, 5.83 mmol) in toluene (50 mL) to give the product as a green solid (1.32 g, 62%). $R_f$ [$CHCl_3$–EtOH (9:1)] = 0.53. $^1$H NMR $\delta$ 9.60–9.63 (m, 8 H, Pc–H$_\alpha$), 8.32–8.34 (m, 8 H, Pc–H$_\beta$), 3.54–3.72 (m, *ca.* 84 H, $CH_2$), 3.44 (vt, $J$ = 4.8 Hz, 4 H, $CH_2$), 3.37 (s, 6 H, Me), 3.20 (vt, $J$ = 4.8 Hz, 4 H, $CH_2$), 2.95 (vt, $J$ = 4.8 Hz, 4 H, $CH_2$), 2.43 (vt, $J$ = 4.8 Hz, 4 H, $CH_2$), 1.65 (vt, $J$ = 4.8 Hz, 4 H, $CH_2$), 0.37 (vt, $J$ = 5.4 Hz, 4 H, $CH_2$), −1.92 (vt, $J$ = 5.4 Hz, 4 H, $CH_2$); MS (MALDI-TOF) isotopic clusters peaking at $m/z$ 2010.1 (calcd for $M^+$: 2012.0) and 1276.2 {calcd for $[M - O(CH_2CH_2O)_nMe]^+$: 1275.6} for $n$ = 16.

**Si(PcCl$_8$)(PEG$_{750}$)$_2$ (4c).** By using the above procedure, **3b** (0.10 g, 0.11 mmol) was treated with $PEG_{750}$ methyl ether (average $M_n \approx 750$; 0.19 g, *ca.* 0.3 mmol) and NaH (25 mg, 1.04 mmol) in toluene (30 mL) to give the product as a green solid (0.14 g, 55%). $R_f$ [$CHCl_3$–EtOH (9:1)] = 0.60. $^1$H NMR $\delta$ 9.64 (s, 8 H, Pc–H$_\alpha$), 3.54–3.64 (m, *ca.* 80 H, $CH_2$), 3.47–3.49 (m, 4 H, $CH_2$), 3.40–3.42 (m, 4 H, $CH_2$), 3.37 (s, 6 H, Me), 3.26–3.28 (m, 4 H, $CH_2$), 3.05–3.07 (m, 4 H, $CH_2$), 2.56–2.58 (m, 4 H, $CH_2$), 1.80–1.83 (m, 4 H, $CH_2$), 0.43 (vt, $J$ = 6.0 Hz, 4 H, $CH_2$), −1.94 (vt, $J$ = 6.0 Hz, 4 H, $CH_2$); MS (MALDI-TOF) isotopic clusters peaking at $m/z$ 2295.5 (calcd for $M^+$: 2286.7) and 1550.7 {calcd for $[M - O(CH_2CH_2O)_nMe]^+$ 1551.2} for $n$ = 16.

**Si(PcBr$_8$)(PEG$_{750}$)$_2$ (4d).** By using the above procedure, **3c** (0.14 g, 0.11 mmol) was treated with $PEG_{750}$ methyl ether (average $M_n \approx 750$; 0.28 g, *ca.* 0.4 mmol) and NaH (25 mg, 1.04 mmol) in toluene (30 mL) to give the product as a green solid (0.16 g, 54%). $R_f$ [$CHCl_3$–EtOH (9:1)] = 0.45. $^1$H NMR $\delta$ 9.83 (s, 8 H, Pc–H$_\alpha$), 3.58–3.64 (m, *ca.* 80 H, $CH_2$), 3.54–3.56 (m, 4 H, $CH_2$), 3.48–3.50 (m, 4 H, $CH_2$), 3.38 (s, 6 H, Me), 3.27–3.29 (m, 4 H, $CH_2$), 3.05–3.07 (m, 4 H, $CH_2$), 2.55–2.57 (m, 4 H, $CH_2$), 1.79–1.81 (m, 4 H, $CH_2$), 0.40 (vt, $J$ = 6.0 Hz, 4 H, $CH_2$), −1.94 (vt, $J$ = 6.0 Hz, 4 H, $CH_2$); MS (MALDI-TOF) isotopic clusters peaking at $m/z$ 2666.0 (calcd for $[M + Na]^+$: 2665.2) and 1904.7 {calcd for $[M - O(CH_2CH_2O)_nMe]^+$: 1906.9} for $n$ = 16.

**4b-BSA conjugate.** A solution of **4b** in THF–EtOH (4:1; 1.4 mL, 2.1 mM) was added dropwise to a solution of BSA (40 mL, 3.6 μM) in Tris-HCl buffer. The mixture with a molar ratio of **4b**:BSA of 20 was stirred at ambient temperature overnight, then chromatographed on a G-100 Sephadex column (Sigma, dry bead diameter = 40–120 μM; 1.8 × 21 cm) using 20 mM aqueous $NH_4HCO_3$ as eluent. The conjugate collected as the first blue fraction was lyophilised to remove $NH_4HCO_3$ and water. The protein content was determined with the Bio-Rad protein assay kit using BSA as standard.[16] The phthalocyanine concentration was calculated from the Q band absorbance in a diluted DMF solution ($\varepsilon_{672}$ for [**4b**] = $2.1 \times 10^5$ $M^{-1}$ $cm^{-1}$).

### *In vitro* studies

For *in vitro* studies, a series of phthalocyanine-containing solutions were first prepared.[12] (*a*) A 2 mM solution of **4b** in THF–EtOH (4:1) was diluted with PBS to give a 80 μM solution. After passing through a 0.45 μm filter, the solution was further diluted with the following medium to give a series of solutions with different concentrations of **4b**. (*b*) A solution of **4b**-BSA conjugate in PBS was prepared. The concentration of **4b** was adjusted to 8 μM as monitored by the Q band absorbance in DMF ($\varepsilon_{672} = 2.1 \times 10^5$ $M^{-1}$ $cm^{-1}$). This solution was then diluted with the medium to appropriate concentrations. (*c*) For studies using Cremophor EL emulsions, 2 mM solutions of **4b–d** were diluted to 80 μM with a *ca.* 0.01 M aqueous solution of Cremophor EL (Sigma, 0.5 g in 100 mL of water). The solutions were clarified with a 0.45 μm filter, then diluted with the medium to appropriate concentrations.

The HepG2 human hepatocarcinoma cells and J774 mouse mammary tumour cells (both from ATCC) were maintained in RPMI medium 1640 (Life Technologies) supplemented with 10% fetal calf serum (Invitrogen). About $2 \times 10^4$ (for HepG2) or $3 \times 10^4$ (for J774) cells per well in this medium were inoculated in 96-multiwell plates and incubated overnight at 37 °C under 5% $CO_2$. The cells were rinsed with PBS and incubated with 100 μL of the above solutions for 2 h under the same conditions. The cells were then rinsed again with PBS and re-fed with 100 μL of the growth medium before being illuminated at ambient temperature. The light source consisted of a 300 W halogen lamp, a water tank for cooling and a colour glass filter (Newport), cut-on 610 nm. The fluence rate ($\lambda$ > 610 nm) was 40 mW $cm^{-2}$. An illumination of 20 min led to a total fluence of 48 J $cm^{-2}$.

Cell survival was determined by means of the colourimetric MTT assay.[23] After illumination, the cells were incubated at 37 °C under 5% $CO_2$ overnight. An MTT (Sigma) solution in PBS (50 μL, 3 mg $mL^{-1}$) was added to each well followed by incubation for 2 h (for HepG2) or 5 h (for J774) under the same environment. A solution of sodium dodecyl sulfate (SDS; Sigma) in 0.04 M HCl(aq) (100 μL, 10% by weight) was then added to each well. The plate was incubated in a 60 °C

oven for 30 min, then 80 μL of *iso*-propanol was added to each well. The plate was agitated on a Bio-Rad microplate reader at ambient temperature for 20 s before the absorbance at 540 nm of each well was taken. The average absorbance of the blank wells, which did not contain the cells, was subtracted from the readings of the other wells. The cell survival was then determined by the equation: Cell Survival (%) = $[\Sigma(A_i/\bar{A}_{\text{control}} \times 100)]/n$, where $A_i$ is the absorbance of the $i$th data ($i = 1, 2, \ldots, n$), $\bar{A}_{\text{control}}$ is the average absorbance of the control wells, in which the phthalocyanine was absent, and $n$ ($\geq 3$) is the number of data points.

### Cell uptake

HepG2 cells were plated at a density of $1 \times 10^6$ cells per well in 6-multiwell plates in the growth medium (5 mL in each well). Following an overnight incubation, the medium was removed and the cells were rinsed with PBS, then incubated with 5 mL of a 2 μM phthalocyanine dilution in the medium for 2 h. The cells were then rinsed with PBS and re-fed with an SDS solution in 0.04 M HCl(aq) (0.5 mL per well, 10% by weight). The plate was incubated in a 60 °C oven for 1 h, then 0.5 mL of *iso*-propanol and 2 mL of DMF were added to each well. The solution was transferred to a 2 mL test tube, which was sonicated and centrifuged. The absorption spectrum of the solution was recorded, from which the concentration of the phthalocyanine could be determined by the Q band absorbance ($\varepsilon_{672} = 2.1 \times 10^5$ $M^{-1}$ $cm^{-1}$ for **4b**, $\varepsilon_{679} = 2.9 \times 10^5$ $M^{-1}$ $cm^{-1}$ for **4c**, $\varepsilon_{682} = 1.7 \times 10^5$ $M^{-1}$ $cm^{-1}$ for **4d**). Each experiment was repeated two times.

### Microscopic studies

Before the MTT assay, the cells in the 96-multiwell plates were viewed with a Zeiss Axiovert 135 microscope (200×) and the photographs were taken with a Nikon D-100 digital camera. For the fluorescence imaging study, about $6 \times 10^4$ HepG2 cells in the medium (0.6 mL) were loaded on a coverslip and incubated overnight at 37 °C under 5% $CO_2$. After removing the medium, the cells were rinsed with PBS and incubated in the medium containing **4b** in PBS ([**4b**] = 8 μM) for 2 h under the same conditions. The cells were then rinsed again with PBS and viewed with an Olympus $1 \times 70$S8F inverted microscope. The excitation light source (at 380 nm) was provided by a multi-wavelength illuminator (Polychrome IV, TILL Photonics). The emitted fluorescence ($> 520$ nm) was collected using a digital cooled CCD camera (Quantix, Photometrics). Images were digitised and analysed using MetaFluor V.6.0 (Universal Imaging).

## Acknowledgements

We thank Prof. Dominic Chan, Yi-Man Fung and Prof. Zongwei Cai for the mass spectrometric measurements. The Croucher Foundation is acknowledged for a Chinese Visitorship to Dr. J.-D. Huang. This work was supported by The Chinese University of Hong Kong (Direct Grant 2002–03), the Natural Science Foundation of China (Grant No. 20201005) and the Foundation for University Key Teachers by the Ministry of Education, China.

## References

1 (*a*) R. Bonnett, *Chemical Aspects of Photodynamic Therapy*, Gordon and Breach, Amsterdam, 2000; (*b*) I. J. MacDonald and T. J. Dougherty, *J. Porphyrins Phthalocyanines*, 2001, **5**, 105; (*c*) N. L. Oleinick, R. L. Morris and I. Belichenko, *Photochem. Photobiol. Sci.*, 2002, **1**, 1; (*d*) M. B. Vrouenraets, G. W. M. Visser, G. B. Snow and G. A. M. S. van Dongen, *Anticancer Res.*, 2003, **23**, 505.
2 (*a*) H. Ali and J. E. van Lier, *Chem. Rev.*, 1999, **99**, 2379; (*b*) R. Bonnett, *J. Heterocycl. Chem.*, 2002, **39**, 455.
3 (*a*) E. A. Lukyanets, *J. Porphyrins Phthalocyanines*, 1999, **3**, 424; (*b*) C. M. Allen, W. M. Sharman and J. E. van Lier, *J. Porphyrins Phthalocyanines*, 2001, **5**, 161; (*c*) A. C. Tedesco, J. C. G. Rotta and C. N. Lunardi, *Curr. Org. Chem.*, 2003, **7**, 187.
4 (*a*) *Poly(ethylene glycol) Chemistry and Biological Applications*, eds. J. M. Harris and S. Zalipsky, American Chemical Society, Washington, DC, 1997; (*b*) G. Molineux, *Cancer Treatment Rev.*, 2002, **28**, 13; (*c*) R. B. Greenwald, Y. H. Choe, J. McGuire and C. D. Conover, *Adv. Drug Delivery Rev.*, 2003, **55**, 217.
5 (*a*) S. W. Young, K. W. Woodburn, M. Wright, T. D. Mody, Q. Fan, J. L. Sessler, W. C. Dow and R. A. Miller, *Photochem. Photobiol.*, 1996, **63**, 892; (*b*) F. Mitzel, S. FitzGerald, A. Beeby and R. Faust, *Chem. Commun.*, 2001, 2596; (*c*) F. Mitzel, S. FitzGerald, A. Beeby and R. Faust, *Chem. Eur. J.*, 2003, **9**, 1233.
6 (*a*) P. Westermann, T. Glanzmann, S. Andrejevic, D. R. Braichotte, M. Forrer, G. A. Wagnieres, P. Monnier, H. van den Bergh, J.-P. Mach and S. Folli, *Int. J. Cancer*, 1998, **76**, 842; (*b*) R. Hornung, M. K. Fehr, J. Monti-Frayne, B. J. Tromberg, M. W. Berns and Y. Tadir, *Br. J. Cancer*, 1999, **81**, 631; (*c*) H.-B. Ris, T. Krueger, A. Giger, C. K. Lim, J. C. M. Stewart, U. Althaus and H. J. Altermatt, *Br. J. Cancer*, 1999, **79**, 1061; (*d*) R. Hornung, M. K. Fehr, H. Walt, P. Wyss, M. W. Berns and Y. Tadir, *Photochem. Photobiol.*, 2000, **72**, 696; (*e*) T. Reuther, A. C. Kübler, U. Zillmann, C. Flechtenmacher and H. Sinn, *Lasers Surg. Med.*, 2001, **29**, 314; (*f*) T. Krueger, H. J. Altermatt, D. Mettler, B. Scholl, L. Magnusson and H.-B. Ris, *Lasers Surg. Med.*, 2003, **32**, 61.
7 (*a*) G. J. Clarkson, A. Cook, N. B. McKeown, K. E. Treacher and Z. Ali-Adib, *Macromolecules*, 1996, **29**, 913; (*b*) G. J. Clarkson, B. M. Hassan, D. R. Maloney and N. B. McKeown, *Macromolecules*, 1996, **29**, 1854; (*c*) T. Toupance, P. Bassoul, L. Mineau and J. Simon, *J. Phys. Chem.*, 1996, **100**, 11 704.
8 (*a*) C. Bellemo, G. Jori, B. D. Rihter, M. E. Kenney and M. A. J. Rodgers, *Cancer Lett.*, 1992, **65**, 145; (*b*) N. Brasseur, R. Ouellet, C. La Madeleine and J. E. van Lier, *Br. J. Cancer*, 1999, **80**, 1533.
9 (*a*) E. Allémann, N. Brasseur, O. Benrezzak, J. Rousseau, S. V. Kudrevich, R. W. Boyle, J.-C. Leroux, R. Gurny and J. E. van Lier, *J. Pharm. Pharmacol.*, 1995, **47**, 382; (*b*) J. C. Leroux, E. Allémann, F. DeJaeghere, E. Doelker and R. Gurny, *J. Controlled Release*, 1996, **39**, 339; (*c*) E. Allémann, J. Rousseau, N. Brasseur, S. V. Kudrevich, K. Lewis and J. E. van Lier, *Int. J. Cancer*, 1996, **66**, 821; (*d*) A. Gijsens, A. Derycke, L. Missiaen, D. de Vos, J. Huwyler, A. Eberle and P. de Witte, *Int. J. Cancer*, 2002, **101**, 78.
10 (*a*) T. Ngai, G. Zhang, X.-Y. Li, D. K. P. Ng and C. Wu, *Langmuir*, 2001, **17**, 1381; (*b*) Z. Sheng, X. Ye, Z. Zheng, S. Yu, D. K. P. Ng, T. Ngai and C. Wu, *Macromolecules*, 2002, **35**, 3681.
11 A preliminary communication has appeared reporting the preparation and photophysical properties of three of these compounds (**4b–d**): P.-C. Lo, S. Wang, A. Zeug, M. Meyer, B. Röder and D. K. P. Ng, *Tetrahedron Lett.*, 2003, **44**, 1967.
12 To simplify the reporting of data and to facilitate comparison, the molecular weights of **4a–d** were estimated by assuming the mass of the polymeric fragments $PEG_{550}$ and $PEG_{750}$ methyl ether to be exactly 550 and 750, respectively.
13 (*a*) J. Vacus and J. Simon, *Adv. Mater.*, 1995, **7**, 797; (*b*) M. Kimura, K. Nakada, Y. Yamaguchi, K. Hanabusa, H. Shirai and N. Kobayashi, *Chem. Commun.*, 1997, 1215; (*c*) A. C. H. Ng, X.-Y. Li and D. K. P. Ng, *Macromolecules*, 1999, **32**, 5292.
14 W. Spiller, H. Kliesch, D. Wöhrle, S. Hackbarth, B. Röder and G. Schnurpfeil, *J. Porphyrins Phthalocyanines*, 1998, **2**, 145.
15 G. Stehle, A. Wunder, H. H. Schrenk, G. Hartung, D. L. Heene and H. Sinn, *Anti-Cancer Drugs*, 1999, **10**, 785.
16 M. M. Bradford, *Anal. Biochem.*, 1976, **72**, 248.
17 N. Brasseur, R. Langlois, C. La Madeleine, R. Ouellet and J. E. van Lier, *Photochem. Photobiol.*, 1999, **69**, 345.
18 D. Wöhrle, M. Eskes, K. Shigehara and A. Yamada, *Synthesis*, 1993, 194.
19 C. C. Leznoff, Z. Li, H. Isago, A. M. D'Ascanio and D. S. Terekhov, *J. Porphyrins Phthalocyanines*, 1999, **3**, 406.
20 C. W. Dirk, T. Inabe, K. F. Schoch, Jr. and T. J. Marks, *J. Am. Chem. Soc.*, 1983, **105**, 1539.
21 D. F. Eaton, *Pure Appl. Chem.*, 1988, **60**, 1107.
22 G. Ferraudi, in *Phthalocyanines-Properties and Applications*, eds. C. C. Leznoff and A. B. P. Lever, VCH, New York, 1989, vol. 1, p. 301.
23 MTT = 3-(4,5-dimethyl-2-thiazolyl)-2,5-diphenyl-2*H*-tetrazolium bromide: H. Tada, O. Shiho, K. Kuroshima, M. Koyama and K. Tsukamoto, *J. Immunol. Methods*, 1986, **93**, 157.